Pure & Appl. Chem., Vol. 70, No. 8, pp. 1547–1566, 1998.
Printed in Great Britain.

INTERNATIONAL UNION OF
PURE AND APPLIED CHEMISTRY

MACROMOLECULAR DIVISION

IUPAC WORKING PARTY IV.2.1: STRUCTURE AND PROPERTIES OF COMMERCIAL POLYMERS

RHEOLOGICAL AND MECHANICAL PROPERTIES OF POLY(α-METHYLSTYRENE-*co*-ACRYLONITRILE)/POLY(METHYL METHACRYLATE) BLENDS IN MISCIBLE AND PHASE SEPARATED REGIMES OF VARIOUS MORPHOLOGIES I. CHARACTERIZATION OF CONSTITUENTS, BLEND PREPARATION, AND OVERVIEW ON BLEND MORPHOLOGY

(Technical Report)

Prepared for publication by

H. M. LAUN

BASF Aktiengesellschaft, Polymer Research Division, ZKM - G 201
Ludwigshafen/Rhein, Germany

* *Contributing Members of the Working Party for this report:*

D. Constantin (France), J. Curry (USA), C. Dehennau (Belgium), W. Gleissle (Germany), M. Lecomte (Belgium), J. Lyngaae-Jörgensen (Denmark), J. Stejskal (Czech Republic).

Rheological and mechanical properties of poly(α-methylstyrene-*co*-acrylonitrile)/poly(methyl methacrylate) blends in miscible and phase separated regimes of various morphologies I. Characterization of constituents, blend preparation, and overview on blend morphology

Abstract: For a collaborative blend study the components PαMSAN (M_w = 82 000, 30% acrylonitrile) and PMMA (M_w = 88 000, 5% methylacrylate) were selected to have a similar melt viscosity and elasticity at 210 °C. Their dynamic moduli are identical in the investigated frequency domain except for a constant factor of 0.61 in the relaxation times. Only a small difference of the WLF temperature shift factors is found between 150 and 230 °C. The PαMSAN/PMMA blends show LCST behaviour. Transparent samples were prepared by melt mixing and subsequent squeezing at temperatures ≤ 160 °C. Annealing yields phase separated specimens with various morphologies. This enables to study the influence of phase structure on rheological and mechanical properties for a constant composition. The PαMSAN rich samples have higher cloud point temperatures than their PMMA rich counterparts. RuO_4-stained ultrathin sections of optically transparent blends containing 40% PαMSAN show a distinct microheterogeneity due to ≈10 nm PMMA rich spheres. 65 hours annealing at 150 °C yields 0.1 μm spheres whereas a co-continuous structure is found after 22 h at 170 °C. Temperatures ≥ 200 °C initiate rapid phase separation with a co-continuous structure being formed for the 40/60 and 60/40 blends whereas the 15/85 and 85/15 blends show droplet morphologies. This paper describes the properties of the constituents, reviews the limits of miscibility, and gives an outline of the whole project.

1. INTRODUCTION

1.1 Historic background

A collaborative feasibility study on "Polymer Mixtures with Non-bonding and Bonding Interactions" within IUPAC Working Party IV.2.1 was initiated by the former Working Party chairman H. H. Meyer at the Cranfield meeting in 1988. The concept of polymer mixtures with non-bonding interactions was further developed by L. A. Utracki, author of [1]. He proposed a programme on immiscible/miscible blends for the components PαMSAN = poly (α-methylstyrene-*co*-acrylonitrile) and PMMA = poly (methyl methacrylate). Both are amorphous polymers which are relatively stable in the molten state. For this system blends with a controlled morphology can be prepared, i.e. single phase blends below the cloud point curve and phase separated blends at temperatures above. Cloud point curves of similar blends were available from [2]. BASF Aktiengesellschaft as supplier of PαMSAN also made available a PMMA component having a similar viscosity function as the PαMSAN at 210 °C. Werner & Pfleiderer USA volunteered for compounding of the blends.

1.2 Objective

The joint project aims the preparation of blends of various morphologies but constant composition and to study the influence of the blend structure on the rheological properties. Because of the selection of rheologically similar constituents only differences due to various morphologies should show up. A second objective is to get more insight into how pressure and flow shifts the range of miscibility as well as the kinetics of phase separation. The formation of a variety of morphologies simply by annealing

miscible blends at elevated temperatures and subsequent cooling below T_g also enables a study of the relevance of the type of morphology on mechanical properties of the blends. A fracture mechanics study on the same system is to be found in [3].

In this introductory paper we present the characterization of the PαMSAN and PMMA constituents, the preparation of miscible blends as well as an overview on phase separation by annealing. More detailed studies on

- Limits of miscibility in the quiescent state and during shear flow [4]
- Manifestation of the interface in oscillatory shear flow
- Morphological changes in simple flow situations and elementary processing steps
- Influence of morphology on mechanical properties
- Critical comparison of rheology data for PαMSAN from various laboratories

being also part of the collaborative study are described in separate papers.

1.3 Contributors

The contributors to this collaborative study are listed in **Table 1.** In the following only the abbreviations for the laboratories will be used.

Table 1. List of contributors

Laboratory	Abbreviation	Representative
BASF Aktiengesellschaft Ludwigshafen/Rhein	BASF	H. M. Laun
Werner & Pfleiderer Corporation Ramsey	W&P	J. Curry
TU Karlsruhe	TUK	W. Gleißle
SHELL RESEARCH Louvain-la-Neuve	SHEL	M. Lecomte
DTH Lyngby	DTH	J. Lyngaae-Jorgensen
ENICHEM Polymères Mazingarbe	ENIC	D. Constantin
SOLVAY Brussels	SOLV	C. Dehennau
Inst. Macromolecular Chemistry Prague	IMC	J. Stejskal

1.4 Related literature

Goh *et al.* [2] report cloud point curves of PαMSAN/PMMA blends. The PαMSAN component was another batch of the same product as studied here. For a PMMA component of similar molecular weight as in Table 3 (denoted as PMMA-2) they report an asymmetric cloud point curve, the lower critical solution temperature (LCST) being 185 °C for 20% PαMSAN. The limiting temperature for miscibility increases with increasing PαMSAN content up to 210 °C for 90% PαMSAN. These data were determined at a heating rate of 10 °C/min. Morphological changes in PSAN/PMMA blends as a function of composition and time were described by L. P. McMaster [5]. Their system shows a LCST of 148 °C for 10% PSAN. Droplet morphology is found for 75% PSAN at 265 °C and co-continuous structures for 25% PSAN at 180 °C and 210 °C.

2. PROPERTIES OF BLEND COMPONENTS

The two blend components are commercial products of BASF Aktiengesellschaft (**Table 2).** Their chemical structure is depicted in **Fig. 1.**

Table 2. Selected blend components

Type	Product Lot-no.	
PαMSAN	Luran KR 2556	62-846-3
PMMA	Lucryl G 77	5695/11

PαMSAN

(Luran KR 2556 , BASF)

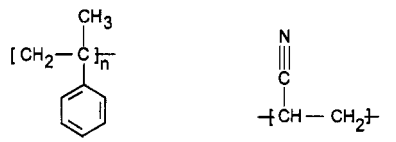

70% α-methylstyrene 30% acrylonitrile

PMMA

(Lucryl G 77 , BASF)

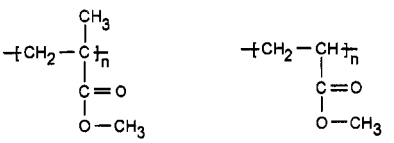

95% methyl methacrylate 5% methyl acrylate

Fig. 1. Chemical composition and trade name of the blend components.

Luran KR 2556 is a copolymer of 70% α-methylstyrene and 30% acrylonitrile by weight. Its average molecular weight determined by light scattering is M_w = 82 000 g/mole (IMC). GPC (PS-calibration) gives M_w/M_n = 2.4 (BASF). A glass transition temperature of T_g = 123 °C is found by BASF. ENIC reports 125 °C. Lucryl G 77 is a copolymer of 95% methyl methacrylate and 5% methyl acrylate by weight. Its average molecular weight determined by light scattering is M_w = 88 000 g/mole (IMC). GPC (PS-calibration) gives M_w/M_n = 2.1 (BASF). The glass transition temperature is T_g = 109 °C (BASF, ENIC). Drying of the samples for 8 h at 80 °C in a vacuum oven is recommended before mechanical or rheological measurements. A summary of the component properties is given in **Table 3**.

Table 3. Component properties

Property	Comments	PαMSAN	PMMA
M_w [g/mol]	LS	82 000	88 000
M_w/M_n	GPC	2.4	2.1
T_g [°C]	DSC	124	109
density	25°C	1.08	1.18
optical appearance	25°C	transparent	clear
melt viscosity η [Pa·s]	210°C, G" = 1000 Pa	$2.29 \cdot 10^4$	$1.35 \cdot 10^4$
melt compliance J_e [Pa^{-1}]	210°C, G" = 1000 Pa	$4.6 \cdot 10^{-5}$	$3.1 \cdot 10^{-5}$

3. MELT RHEOLOGY

3.1 Linear viscoelasticity of the melt

Mastercurves of the dynamic moduli for a reference temperature of 210 °C for PαMSAN from small amplitude oscillatory shear measurements (BASF) are shown in **Fig. 2a**. A Rheometrics Dynamic Spectrometer RDS2 with plate-plate geometry (radius 12.5 mm, gap 1 mm) and shear amplitude $\hat{\gamma} = 0.01$ was used. The original frequency sweeps were performed from 100 to 0.1 rad/s in the temperature range of 150 °C to 270 °C. Both a horizontal and vertical shift was applied by the Rheometrics RHIOS 3.01 software, the resulting temperature shift factor a_T (see below) being the horizontal shift factor for $tan\ \delta = G''/G'$ (G' storage modulus, G'' loss modulus, δ phase angle) . **Fig. 2b** shows the corresponding mastercurve of the dynamic moduli for PMMA (BASF). Here, a strain amplitude of 0.05 was used.

A zero shear rate viscosity η_o and steady state compliance J_e^o may be evaluated from the terminal zone at low frequencies where $G'' \sim \omega$ and $G' \sim \omega^2$. To avoid some arbitrariness in defining the terminal zone from the measurements, however, it is preferred to evaluate a melt viscosity η and melt compliance J_e at the angular frequency at which the loss modulus reaches a constant value of $G'' = 1000$ Pa:

$$\eta \equiv \left.\frac{G''}{\omega}\right|_{G''\,=\,1000\ \mathrm{Pa}} \qquad \text{and} \qquad J_e \equiv \left.\frac{G'}{G''^2}\right|_{G''\,=\,1000\ \mathrm{Pa}} \tag{1}$$

The values determined from the mastercurves (Figs. 2a,b), $\eta = 2.4 \cdot 10^4$ Pas and $J_e = 4.1 \cdot 10^{-5}$ Pa^{-1} (PαMSAN) respectively $\eta = 1.3 \cdot 10^4$ Pas and $J_e = 2{,}9 \cdot 10^{-5}$ Pa^{-1} (PMMA), are in good agreement with the data of Table 3 representing the average from various rheometers (see below).

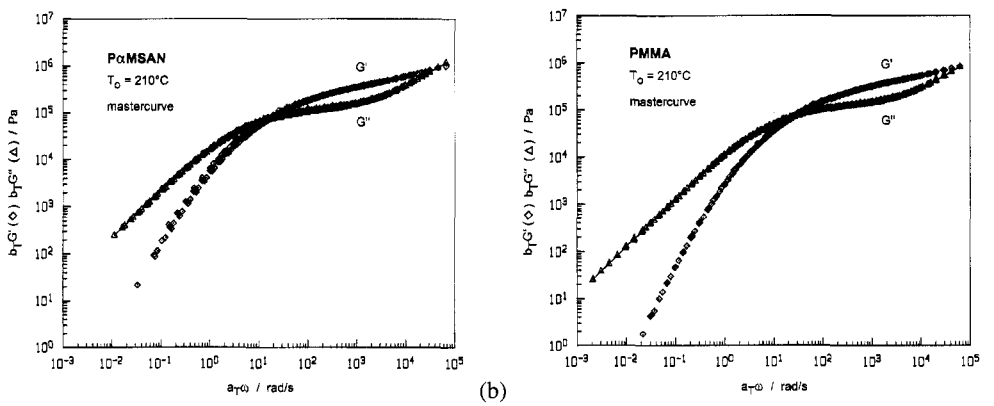

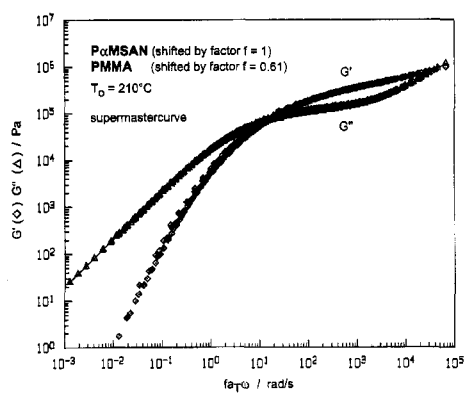

Fig. 2. (a) Dynamic moduli mastercurve of the PαMSAN component for a reference temperature of 210 °C (BASF). (b) Dynamic moduli mastercurve of the PMMA component for a reference temperature of 210 °C (BASF). (c) Super-mastercurve obtained by shifting the PMMA-mastercurve to smaller frequencies (factor $f = 0.61$).

Both mastercurves exhibit quite similar shapes. In fact, the data from the two melts coincide on a super-mastercurve (**Fig. 2c**) if the PMMA data are shifted by an additional factor $f = 0.61$ along the

frequency axis (reduced angular frequency $f \cdot a_T \cdot \omega$). This results means the relaxation time spectra of the two melts at 210 °C are similar, the relaxation times of PMMA being by a factor $1/f$ shorter than those of PαMSAN, however.

3.2 Temperature dependence

The temperature shift factors a_T from the mastercurves (Figs. 2a,b) are plotted in **Fig. 3**.

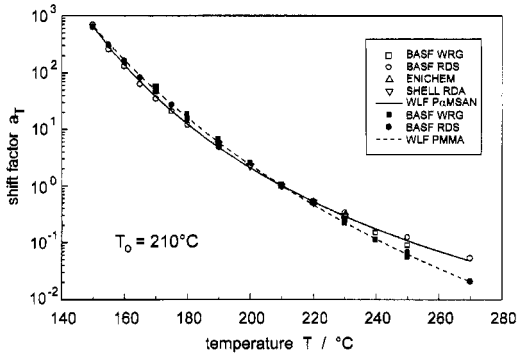

Fig. 3. Temperature shift factors from various laboratories and fit by the WLF-equation.

This diagram also contains shift factors determined by other contributing laboratories. Note that the temperature dependencies of the two melts are very similar in the range of 150 °C to 230 °C. The drawn lines represent the fit by the WLF-equation

$$a_T = \exp \frac{-c_1 (T - T_o)}{c_2 + (T - T_o)} \tag{2}$$

The parameters c_1 and c_2 are listed in **Table 4**.

Table 4. WLF parameters and apparent activation energies E_a from Fig. 3

	T_g [°C]	T_o [°C]	c_1	c_2 [°C]	E_a(170 °C) [kJ/mol]	E_a(210 °C) [kJ/mol]	E_a(230 °C) [kJ/mol]
PαMSAN	124	210	11.48	167.1	194	133	115
PMMA	109	210	19.49	240.8	190	157	145

This table also gives apparent activation energies E_a calculated as

$$E_a = -R \frac{\mathrm{d} \ln a_T}{\mathrm{d} (1/T)} = R \frac{c_1 c_2 T^2}{[c_2 + (T - T_o)]^2} \tag{3}$$

for temperatures of 170 °C, 210 °C, and 230 °C. In addition to the reference temperature T_o = 210 °C the WLF curves intersect at 150 °C. Because of this the PαMSAN melt exhibits the higher apparent activation energy at 170 °C whereas E_a is smaller than that of PMMA at 210 °C. It should also be noted that the relatively high values of the apparent activation energies make it necessary to carefully control the actual temperature when comparing results from various laboratories.

3.3 Stability of the melt

The thermal stability of the melts was investigated in small amplitude oscillatory shear by measuring G' and G'' at a constant frequency of 1 rad/s as a function of the residence time at temperatures between 160 °C and 240 °C (SHEL). **Table 5** summarizes the relative changes of the moduli for an increase of the

residence times from 20 to 120 min. The melts are fairly stable up to 220 °C. At 240 °C the decrease of the storage modulus within 100 min reaches 7.5% (PαMSAN) and 15% (PMMA).

Table 5. Thermal stability of melts at ω = 1 rad/s (SHEL)

	PαMSAN		PMMA	
T [°C]	$\Delta G'$ [%]	$\Delta G''$ [%]	$\Delta G'$ [%]	$\Delta G''$ [%]
160	+1.0	+0.8	−3.0	−3.0
180	−1.3	−1.6	−0.5	−0.8
200	+0.4	+0.0	−0.3	−0.8
220	−1.2	−1.2	−4.0	−4.0
240	−7.5	−5.5	−15	−19

3.4 Comparison of dynamic moduli from various rheometers

A comparison of the dynamic moduli from various rheometers of the BASF laboratory at 210 °C is shown in **Fig. 4a** (PαMSAN) and **Fig. 4b** (PMMA).

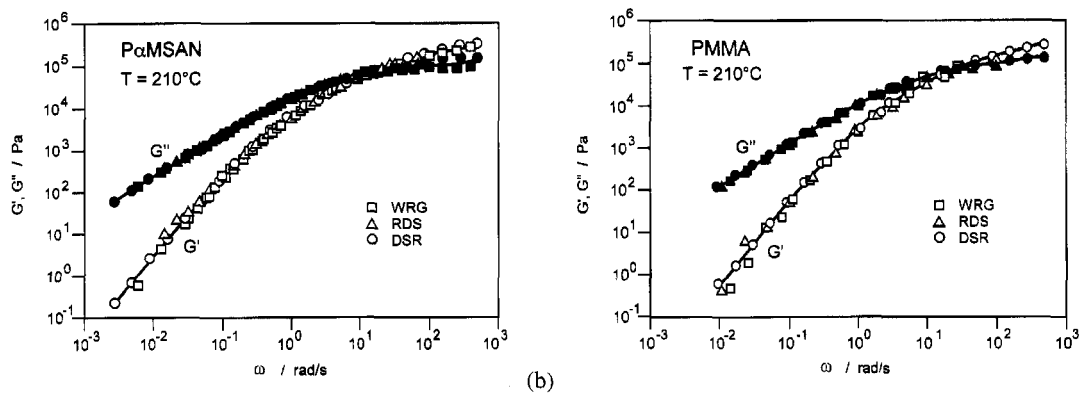

Fig. 4 (a) Dynamic moduli of PαMSAN measured at 210 °C by means of three different rheometers. Full lines represent the fit by the discrete spectrum listed in Table 6. (b) Dynamic moduli of PMMA measured at 210 °C by means of three different rheometers. Full lines represent the fit by the discrete spectrum listed in Table 6.

RDS denotes the above mentioned Rheometrics RDS2. Results from the Rheometrics Dynamic Stress Rheometer using plate-plate geometry (radius 12.5 mm, gap 1 mm) are denoted by DSR. WRG stands for the modified Weissenberg-Rheogoniometer [6] with cone-plate geometry (radius 25 mm, cone angle 4.6°). The agreement is encouraging. Sources of some discrepancies in detail may be slight differences in the true sample temperature, transducer or instrument compliance for the high modulus range (high frequency), and resolution limits of the phase angle measurement for small G'/G'' ratios (small frequencies). The full lines represent the fit of the data by a discrete relaxation time spectrum using the programme IRIS [7]:

$$G' = \sum_i G_i \frac{\omega^2 \lambda_i^2}{1+\omega^2\lambda_i^2} \quad \text{and} \quad G'' = \sum_i G_i \frac{\omega\lambda_i}{1+\omega^2\lambda_i^2} \tag{4}$$

The relaxation times λ_i and relaxation strengths G_i are listed in **Table 6**.

Table 6. Discrete relaxation spectra for 210 °C (BASF)

	PαMSAN		PMMA	
i	λ_i [s]	G_i [Pa]	λ_i [s]	G_i [Pa]
1	$1.616 \cdot 10^{-3}$	$2.340 \cdot 10^{5}$	$2.256 \cdot 10^{-3}$	$2.510 \cdot 10^{5}$
2	$1.871 \cdot 10^{-2}$	$1.326 \cdot 10^{5}$	$1.936 \cdot 10^{-2}$	$1.066 \cdot 10^{5}$
3	$1.339 \cdot 10^{-1}$	$5.993 \cdot 10^{4}$	$9.177 \cdot 10^{-2}$	$4.775 \cdot 10^{4}$
4	$9.122 \cdot 10^{-1}$	$1.084 \cdot 10^{4}$	$5.130 \cdot 10^{-1}$	$1.118 \cdot 10^{4}$
5	$8.816 \cdot 10^{0}$	$2.365 \cdot 10^{2}$	$3.908 \cdot 10^{0}$	$1.846 \cdot 10^{2}$

The discrete spectrum may be used to calculate the average viscosity functions of the two melts for 210 °C by using the Cox–Merz-rule [8],

$$\eta(\dot{\gamma}) = \left|\eta^*(\omega)\right| \quad \text{for} \quad \dot{\gamma} = \omega, \tag{5}$$

$|\eta^*|$ being the absolute value of the complex viscosity and η the steady shear viscosity at shear rate $\dot{\gamma}$. The resulting viscosity function is plotted in **Fig. 5**.

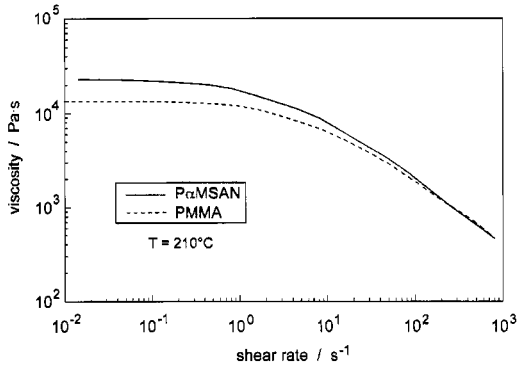

Fig. 5. Viscosity functions calculated from the relaxation time spectra in Table 6 using the Cox-Merz-rule.

The zero shear viscosity may be calculated from the spectrum by

$$\eta_o = \sum_i G_i \lambda_i \tag{6}$$

The resulting zero shear rate viscosity of PαMSAN ($\eta_o = 2.29 \cdot 10^5$ Pas) is by the factor 1.64 higher than that of PMMA ($\eta_o = 1.35 \cdot 10^5$ Pas). At 1000 s^{-1} the viscosity levels are identical. The viscosities and compliances evaluated from the spectra according to Eq. (1) for $G'' = 1000$ Pa are contained in Table 3. They are in good agreement with the values from the mastercurves in Figs. 2a,b. Note that the discrete relaxation spectra in Table 6 represent average dynamic moduli for 210 °C from various rheometers whereas the mastercurves in Figs. 3a,b stem from only one instrument but are based on measurements in a wide temperature range. Thus a spectrum fitted to these mastercurves may yield parameters slightly different from those in Table 6.

4. SURVEY ON THE DOMAIN OF MISCIBILITY

To facilitate the readability of the following sections we present in **Fig. 6** a survey on the domain of miscibility of the PαMSAN/PMMA blends. The origin of the data will be discussed in more detail later in the text. The glass transition temperature T_g as a function of blend composition is represented by squares. Full symbols represent the T_g data on the pure components (Table 3) and of a transparent mixture prepared in the melt (see below). The unfilled squares represent glass transition temperatures

from DSC measured on transparent blends which have been prepared by solution mixing in acetone/water 10/90 and subsequent drying in a vacuum oven at 120 °C (BASF). These samples exhibit a single glass transition temperature.

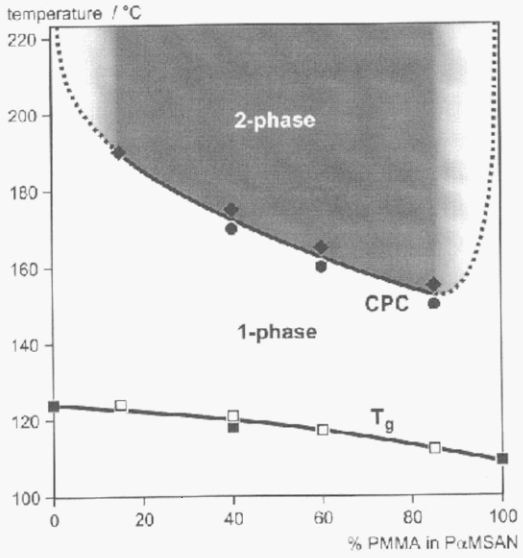

Fig. 6. Limiting temperature for miscibility from annealing investigations and glass transition temperature vs. blend composition (see text).

The cloud point curve (CPC) for blends with PMMA contents between 15% and 85% stems from annealing experiments (circles, compare Table 11) and turbidity investigations on a light microscope (diamonds, compare Table 12). It is obvious from these data that the phase diagram is not symmetrical. The LCST is in the vicinity of 155 °C at roughly 85% PMMA. Since for that composition the distance from T_g is less than 40 °C one may anticipate relatively high viscosities of both components and thus a small speed of phase separation if starting from a homogeneous mixture. For a blend with inverse composition (15% PMMA) the limiting temperature for miscibility is more than 60 °C above T_g.

5. PREPARATION OF BLENDS

5.1 Small scale preparation of homogeneous blends

PMMA is a completely clear sample whereas PαMSAN is transparent with a slight amber-like colour. Blends with high PαMSAN content if prepared in a Brabender kneader at 184 °C applying 6 rpm for 15 min the samples are transparent or translucent (BASF). In the following the mixtures are indicated by the PαMSAN/PMMA content by weight:

PαMSAN/PMMA	optical appearance
85/15	transparent
60/40	translucent
40/60	partially opaque
15/85	milky

When these blends are subsequently squeezed at 160 °C by means of a laboratory press into plaques of 0.3 mm thickness the resulting specimens all appear transparent. It is assumed that the squeeze flow deformation has the effect of a low temperature mixing process where phase separated regions mix again or are at least transformed into a micro heterogeneous phase. This was investigated by transmission electron microscopy (BASF) on RuO_4-stained ultrathin sections. Here, the PαMSAN-rich phase appears

dark. At a magnification of 80.000 (**Fig. 7**) a distinct micro-heterogeneity of the transparent 40/60 blend sample is observed.

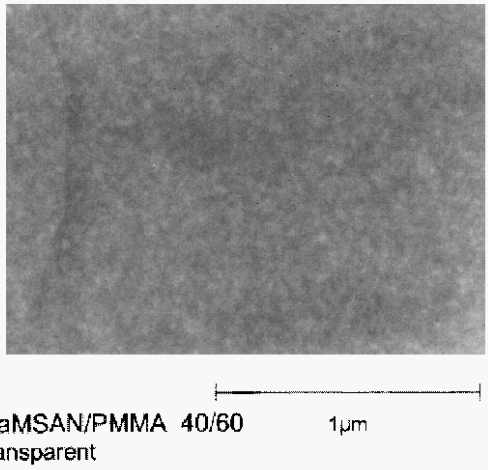

Fig. 7. The transparent plate of the 40/60 blend exhibits a weak microheterogeneity in RuO_4-stained ultrathin sections at high magnification.

The size of bright PMMA-rich domains is in the order of 30 nm. For the transparent mixtures having higher PαMSAN content no such microheterogeneity could be detected. **Fig. 8** shows a DSC diagram on the transparent 60/40 blend (BASF). Only one glass transition at 118 °C, located between the T_g-values of the pure constituents is observed, as expected for a homogeneous mixture.

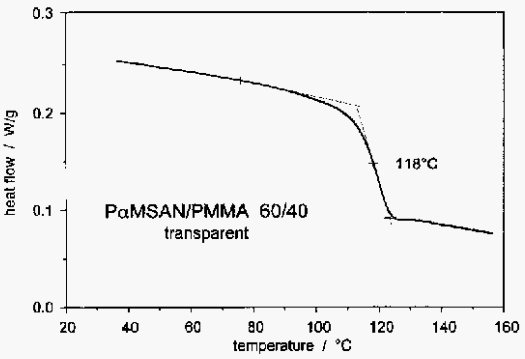

Fig. 8. The transparent plate of the 60/40 blend shows only one glass transition temperature in the DSC trace indicating miscibility .

It was further found that the predominantly clear part of blend strips prepared by extrusion (see W&P samples below) can also be converted to completely transparent samples if squeezed at temperatures $T \leq 160$ °C (BASF). It may be necessary to repeat the squeezing process several times in order to remove originally opaque domains of the sample. **Fig. 9** shows micrographs of RuO_4-stained ultrathin sections of the W&P blends at a magnification of 20.000. Here, the 40/60 blend as well as the blends with higher PαMSAN content appear homogeneous (the micrograph of the 85/15 blend, not shown here, corresponds completely to that of the 60/40 mixture). However, a clear micro phase-separation was found for the 15/85 blend, the size of bright PMMA-rich domains being in the order of 100 nm.

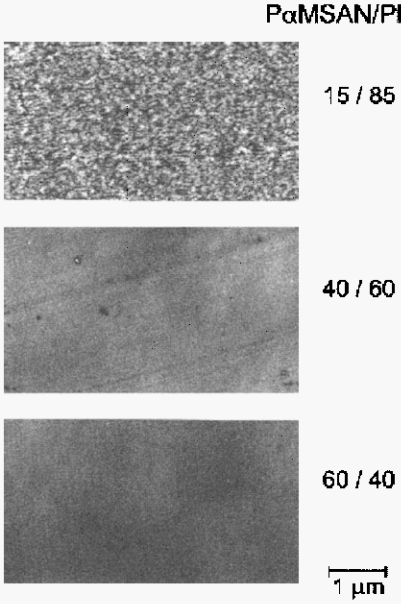

Fig. 9. RuO_4-stained ultrathin sections of the transparent plates for various compositions. The 15/85 blend shows a distinct micro phase separation whereas micrographs with higher PαMSAN content indicate miscibility at the given magnification.

A Brabender Plasticorder was used by DTH to prepare one-phase blends for light scattering experiments: Pellets are manually premixed in a beaker. This mixture is gradually added to the Brabender mixing chamber preheated to 150 °C. The speed of the mixing blades is set to 10 rpm and mixing is continued until a constant torque is reached (5–8 min). After mixing the blends are squeezed in a hydraulic press at 150 °C into 0.5 mm plates. Samples of the pure constituents prepared in the same way to check the possibility of a thermomechanical degradation during preparation of the specimens. GPC measurements using PS-calibration (**Table 7**) indicate, however, that no significant degradation takes place during melt mixing at 150 °C (DTH).

Table 7. Check of degradation during melt mixing at 150 °C (DTH)

	PαMSAN		PMMA	
	no treatment	after mixer	no treatment	after mixer
M_w [10^4 g/mol]	8.50	8.40	10.0	10.3
M_n [10^4 g/mol]	4.20	4.40	4.40	4.60
M_w/M_n	2.01	1.91	2.27	2.25

5.2 Distribution samples preparation by W&P

Pellets were blended in a double cone blender and subsequently dried in a convection oven with desiccated air. Dried pellet mixtures were fed from a single screw volumetric feeder to a ZSK-30 twin screw corotating intermeshing and self wiping plasticating and compounding extruder. In a preliminary compounding test the melt was dropped to a thermally regulated 2 roll mill. The quenched strip was ground in a rotating knife mill. A flow diagram is shown in **Fig. 10**. Initial attempts to extrude sample 50/50 through a die produced swollen strands without melt strength, an indication of poor compatibility. Pressed strands were only slightly milky, indicating fair mixture quality in the single phase region unless single component domains survived the mixing process. Samples 60/40 and 85/15 were extruded through

a slot and quenched on a roll mill. Reducing the extruder RPM was effective to produce clearer strips for the critical 60/40 blend. These highly viscous melts produce high die pressures.

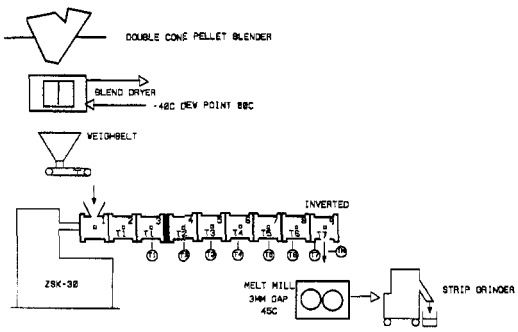

Fig. 10. Flow diagram for the distribution blends preparation at W&P.

The final fabrication conditions are listed in **Table 8**.

Table 8. Fabrication conditions of distributed blends (W&P)

PαMSAN / PMMA	100/0	85/15	60/40	40/60	15/85	0/100
Screw Speed [r.p.m.]	69	50	50	72	112	65
Torque: % of maximum	105	102	113	94	74	108
Calc. mech. power [kW]	1.34	.94	1.04	1.25	1.53	1.38
Throughput rate [lbs/h]	11	7	12	14	19.3	11
Spec. mech. energy [kWh/kg]	0.268	0.297	0.192	0.197	0.175	0.276
product melt temperature [°C]	203	185–200	184–192	194–197	201	203
T1 [°C]	154	158	170	155	155	155
T2 [°C]	157	154	168	155	156	154
T3 [°C]	155	153	171	155	154	155
T4 [°C]	147	152	150	149	149	150
T5 [°C]	151	149	150	149	151	148
T6 [°C]	150	149	150	150	150	150
T7 [°C]	172	169	170	161	170	170
appearance of melt	clear	clear	translucent	milky		clear
appearance of strip	clear	clear	clear	striated milky	cloudy	clear

The ZSK screw design is depicted in **Fig. 11**. Because of the experience with preliminary testing a zero pressure discharge system (an inverted open barrel) was used to feed the mill and critical compositions like 40/60 and 60/40 were prepared at minimal screw speed (torque limited) and rate (feeder limited). It is noteworthy that the compounder discharge melt temperature was not lower despite these measures than in the preliminary testing. Although it was desirable to compound all samples between T_g of the components and the cloud point temperature of the blend, it is clear that this may only have been accomplished for the 85/15 blend. Despite that fact, the finished strips of all samples were mostly clear.

The general observation is that the mixer is resisting the phase separation tendency. Therefore, newly manufactured blends whose discharge temperatures are above the cloud point can appear clear for short periods of time. Whenever a bank is allowed to build in the mill, the blends will cloud. All strips were manufactured without allowing a bank of melt.

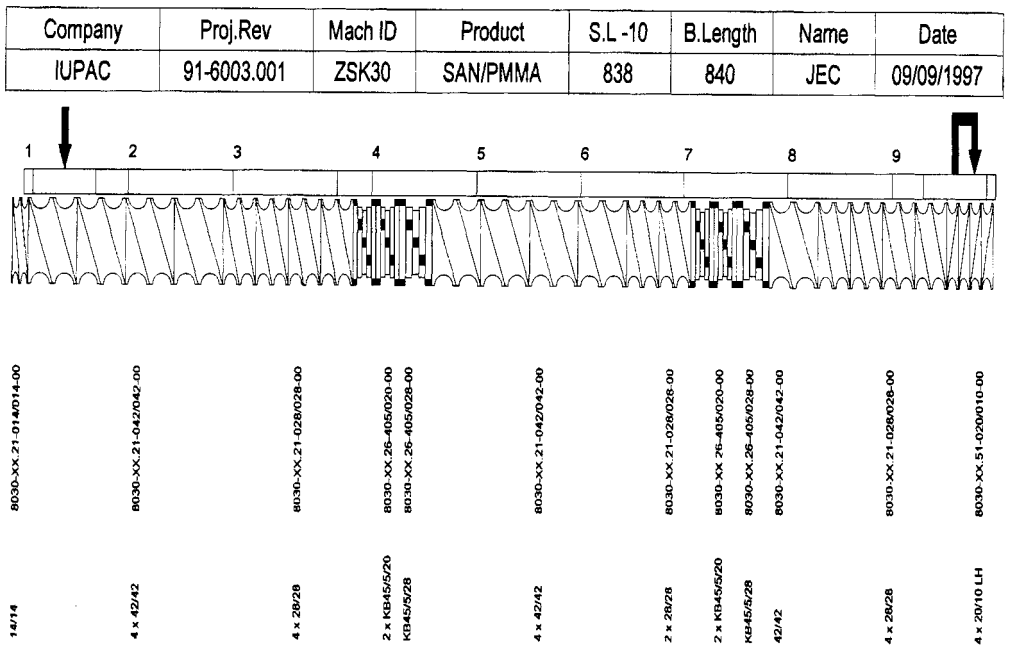

Fig. 11. Schematic of the ZSK 30 design used for blend preparation at W&P.

The reason for the relatively low specific mechanical energy of the 15/85 blend is that the throughput rate is high compared to other samples in an attempt to keep specific energy (drive energy/rate) low and consequently minimize dissipated heat. Conversely, the specific energy of the 85/15 blend is high because the rate is low.

The residence time in the plasticating compounder was investigated for the pure PαMSAN by a pulsed colour tracer. The first indication of colour change occurred after 1 min, a distinct decrease in intensity after 3 min. The colour tracer remained visible even after 14 min.

6. VISCOSITY OF BLENDS

6.1 Oscillatory shear measurements

A comparison of the dynamic moduli of the pure constituents and of the transparent 60/40 PαMSAN/PMMA blend is shown in **Fig. 12** (BASF).

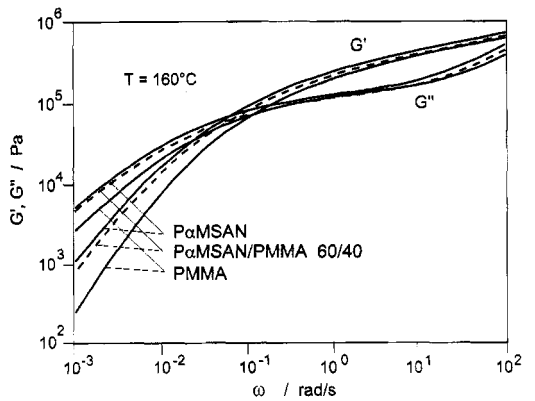

Fig. 12. Dynamic moduli of the pure constituents and of the transparent 60/40 blend at 160 °C (RDS, strain amplitude 0.2).

The low measuring temperature of 160 °C has been chosen, to avoid phase separation during the measurement (see below). Since the temperature shift factors are very similar (compare Fig. 3) for that temperature the relative difference between the moduli of the constituents resembles that at 210 °C. The moduli of the blend lie between those of the components as expected for a homogeneous mixture. However, it is noteworthy that the blend moduli are surprisingly close to those of the pure PαMSAN. It was further found that only in the case of 40/60 and 15/85 blends their moduli approach those of the pure PMMA melt.

Fig. 13 shows the composition dependence of the absolute value of the complex viscosity $|\eta^*|$ at 160°C for three angular frequencies. At 0.1 and 10 rad/s the blend viscosity is practically insensitive to the blend composition since the values of the constituents are comparable. For 0.001 rad/s, however, the higher zero shear rate viscosity of PαMSAN compared to PMMA gives rise to an increase of the blend viscosity with increasing PαMSAN content. Surprisingly, a plateau is reached for ≥40% PαMSAN.

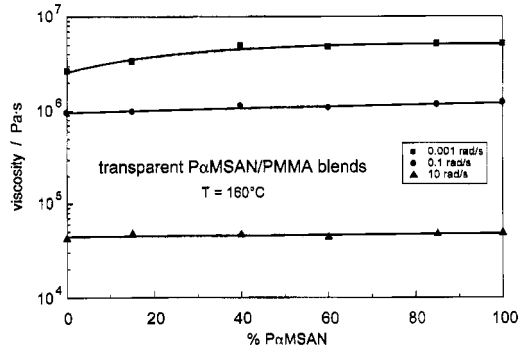

Fig. 13. Composition dependence of the absolute value of the complex viscosity at 160 °C for different angular frequencies (RDS, strain amplitude 0.2).

6.2 Capillary rheometry

Blend viscosities at 210 °C as measured by capillary rheometry (SOLV) are depicted in **Fig. 14** versus composition for several apparent shear rates. Capillaries of radius 0.5 mm and various lengths have been used. The data represent Bagley corrected apparent viscosities. Note that due to the elevated temperature (compare Fig. 6) all blends are in the 2-phase regime at rest. As expected from the very similar high shear rate viscosities of the constituents the blend viscosity remains unaffected by composition at shear rates ≥ 400 s^{-1} whereas a slight increase with growing PαMSAN content is visible at smaller shear rates.

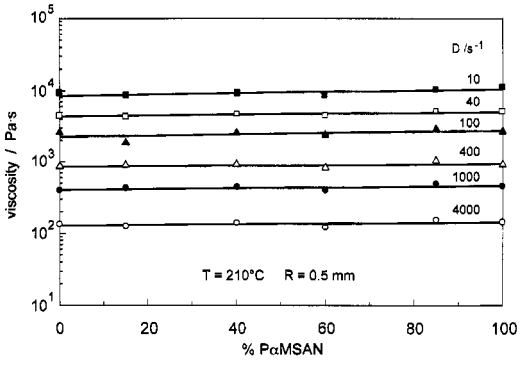

Fig. 14. Composition dependence of the viscosity at 210 °C as measured by capillary rheometry for various shear rates (SOLV).

7. PHASE SEPARATION DURING ANNEALING

7.1 Short time annealing at 220 °C

When the miscible 60/40 blend (squeezed at 160 °C to 1 mm sheet, one single T_g, comp. Fig. 8) is annealed for 5 min at 220 °C the specimen turns opaque indicating phase separation. In the DSC curve, **Fig. 15,** this shows up by two glass transition temperatures of 111 °C and 123 °C being close to the T_g values of the pure constituents (BASF).

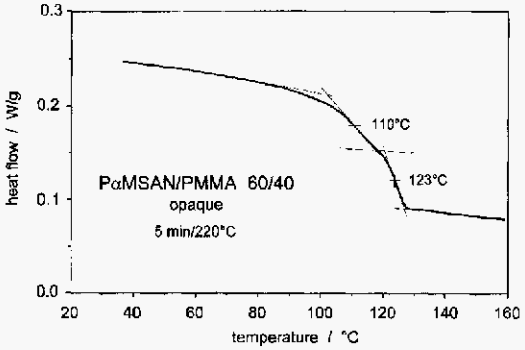

Fig. 15. DSC trace of a phase separated 60/40 blend after 5 min annealing at 210 °C (instrument, heating rate) showing two glass transitions.

Fig. 16 shows the morphology change of the originally transparent blends from Fig. 9 if the specimens are treated for 10 min at 220 °C (BASF). The RuO_4-stained PαMSAN-rich domains appear dark in the micrographs. For the 15/85 blend a droplet morphology with particle diameters up to 350 nm is found. Presumably the annealing took place below the spinodal such that the mechanism of phase separation is nucleation and growth. The 40/60 and 60/40 blends form a co-continuous structure, the strands of the minor phase having a diameter of several μm. Here it is reasonable to assume spinodal decomposition during annealing.

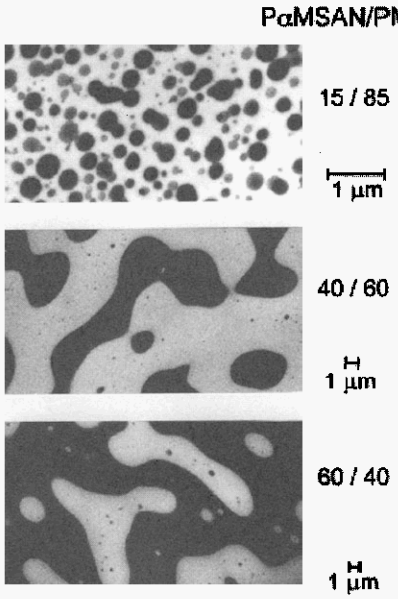

Fig. 16. RuO_4-stained micrographs of phase separated blends after 10 min annealing at 220 °C.

7.2 Long time annealing at 150 °C to 170 °C

The transparent 40/60 blend (compare Fig. 7) if annealed for 65 h at 160 °C becomes slightly opaque. The RuO_4-stained ultrathin section (**Fig. 17,** magnification 80.000) now shows the formation of PMMA-rich spheres of about 0.1 µm diameter (BASF) which hints to a nucleation and growth process. If the originally transparent sample is annealed for 22 h at 170 °C, however, the micrograph (magnification 7.000) clearly indicates that a coarse co-continuous structure is formed by spinodal decomposition.

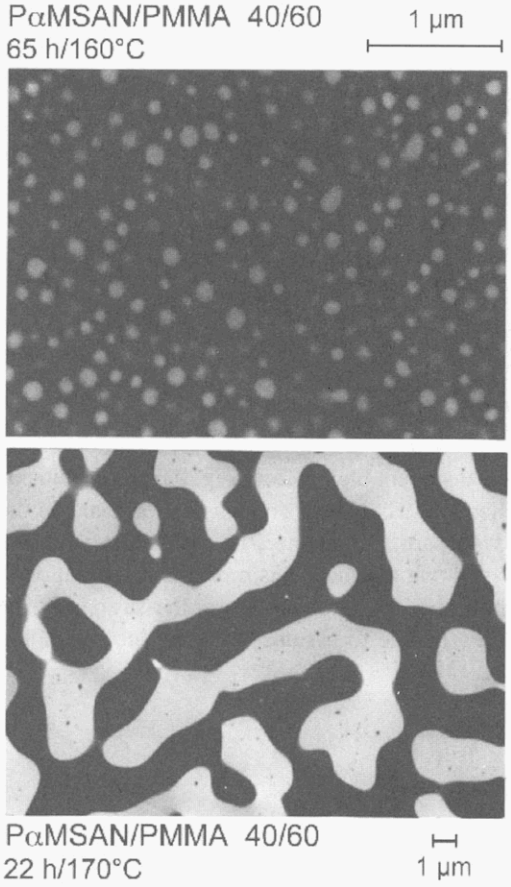

Fig. 17. RuO_4-stained micrographs of the phase separated 40/60 blend after two different annealing treatments.

Table 9 lists for various annealing conditions the optical appearance of blends originally prepared in the Brabender kneader at 184 °C and squeezed to transparent samples.

Table 9. Optical appearance of transparent specimens after annealing (BASF)

PαMSAN / PMMA	75 h /130 °C	65 h / 150 °C	22 h / 170 °C
85/15	–	transparent	transparent
60/40	–	transparent	milky
40/60	transparent	opaque	milky
15/80	translucent	milky	milky

The specimens from Fig. 17 are also contained in this list. According to Fig. 6 it is unlikely that phase separation occurs at 130 °C. Yet annealing for 75 h at 130 °C causes a shift from a transparent to a translucent sample in the case of the PMMA-rich 15/85 blend, whereas no optical change is observed for the 40/60 blend.

The annealing study at 150 °C and 170 °C was duplicated by ENIC (**Table 10**) and the underlying morphological changes investigated by electron microscopy.

Table 10. Morphology of annealed blends (ENIC)

PαMSAN / PMMA	65 h / 150 °C	22 h / 170 °C
85/15	one phase	one phase
60/40	one phase	phase separation PMMA nodules 0.1–0.2 μm
40/60	phase separation beginning some PMMA nodules 0.1–0.15 μm	phase separation two continuous phases size several μm
15/85	phase separation PαMSAN nodules 0.1–0.2 μm	phase separation PαMSAN nodules various sizes

Blend strips distributed by W&P were squeezed at 160 °C to plaques of 0.8 mm thickness. Notched samples were fractured in liquid nitrogen, coated with gold, and examined at the smooth zones near the notch with magnification 20,000 and 7,000. Micrographs are shown in **Fig. 18**. PMMA has a smoother rupture face than PαMSAN which explains the evolution of aspect with the increase in PMMA content.

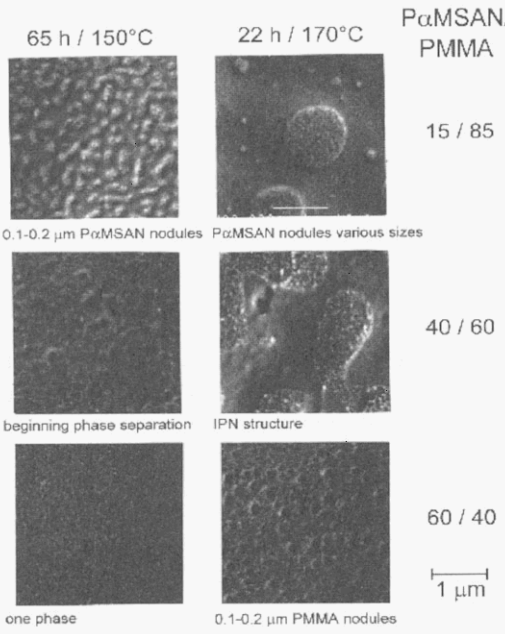

Fig. 18. Micrographs of gold coated fracture surfaces (ENIC) of blends for two different annealing conditions.

An overview of the optical appearance of annealed (originally transparent samples) as a function of annealing time at 150 °C, 160 °C and 170 °C is schematically given in **Fig. 19**.

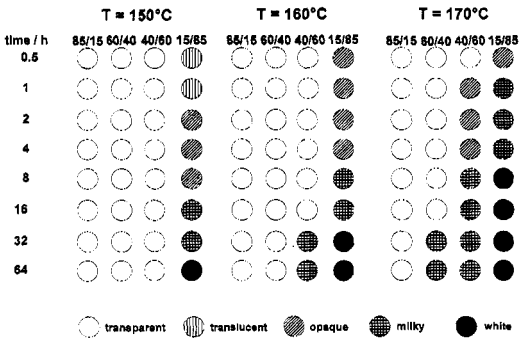

Fig. 19. Optical appearance of originally transparent 1 mm sheets after various annealing times at 150, 160 and 170 °C.

It follows that the 15/85 blends starts to phase separate at 150 °C within a short time, whereas the 85/15 blend does not phase separate at 170 °C (at least as visible by the human eye). A visible phase separation occurs for the 40/60 blend after 32 h at 160 °C and for the 60/40 blend after 32 h at 170 °C. It is obvious, therefore, that the annealing time plays an important role whether morphological changes are to be detected or not. **Table 11** summarizes the temperatures for phase separation T_{ps} resulting from the annealing experiments.

Table 11. Phase separation temperature from annealing experiments

PαMSAN / PMMA	T_{ps} [°C]
85/15	
60/40	170
40/60	160
15/85	≤ 150

7.3 KINETICS OF PHASE SEPARATION

Transparent compression moulded sheets of 0.3 mm thickness were annealed on a hot stage of a light microscope (BASF). During phase separation the transmission of light as determined by a photometer decreases. **Fig. 20** shows the transmission normalised with respect to the initial transmission.

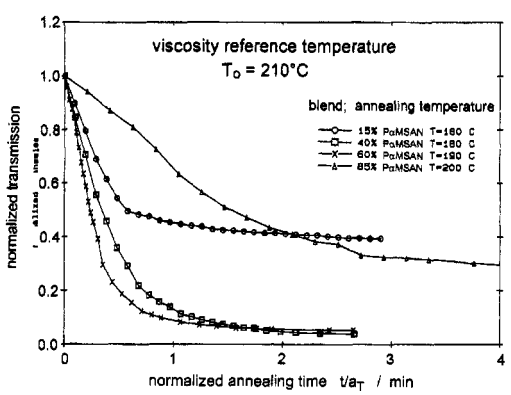

Fig. 20. Transmission change vs. reduced annealing time (reference temperature T_o = 210 °C) of the four blends at differing annealing temperatures.

Different temperatures were chosen for the four blends. To take into account the viscosity change with temperature the time is divided with the temperature shift factor from Fig. 3 (average value of both

constituents) for a reference temperature of 210 °C. For the conditions chosen all blends show a relatively rapid change of transmission due to phase separation. The formation of the droplet morphology in the 15/85 and 85/15 blends yields a transmission reduction by about 60%. The co-continuous structure in the 40/60 and 60/40 blends gives rise to a transmission reduction of more than 90%. Note that even at 200 °C the transmission change for the PαMSAN-rich blend 85/15 is relatively slow.

For a more detailed investigation of the speed of change at various temperatures the transmission measurement was started at a temperature for which hardly a transmission change was observed. This temperature was 160 °C for the 15/85 blend and set to 190 °C for the 85/15 blend. The sample was kept at that very temperature for 3 min and subsequently annealed for another 3 min at a temperature increased by 5 °C. Several temperature steps of 5 °C with 3 min duration each were recorded in series. The resulting normalized transmission is plotted in **Fig. 21a-c** versus the reduced time t/a_T (T_o = 210 °C). The lowest temperature at which a distinct slope of the transmission vs. reduced time is observed is taken as the temperature for start of phase separation. The resulting temperatures are listed in **Table 12**.

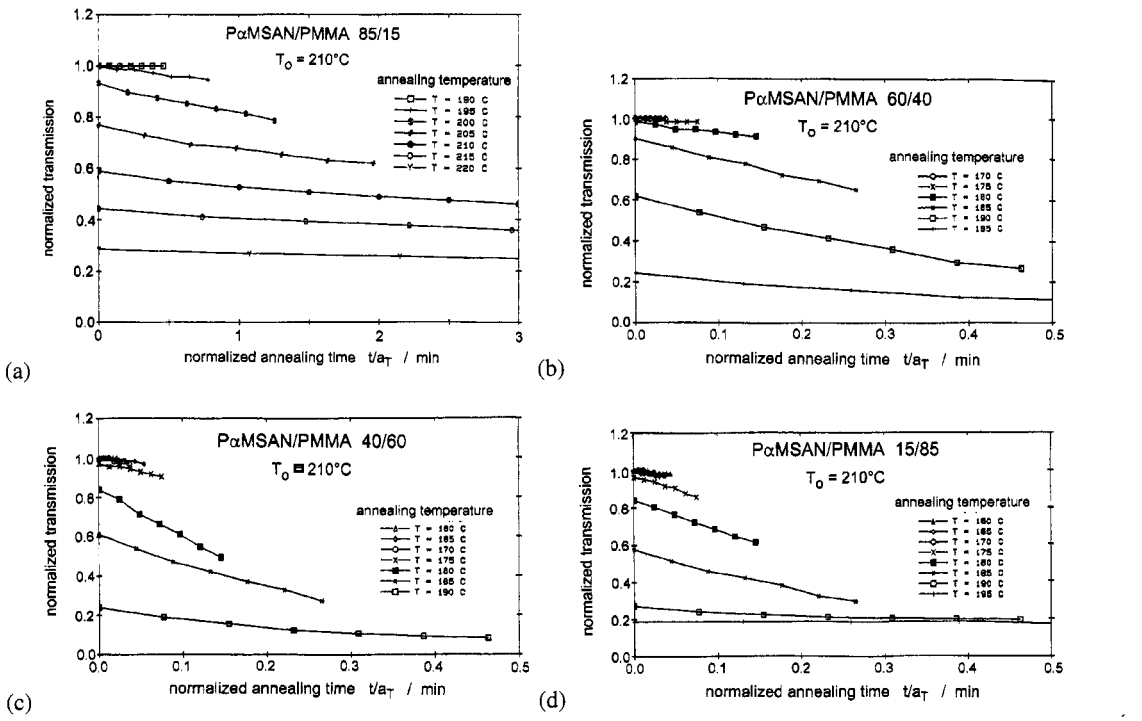

Fig. 21. Transmission change vs reduced annealing time t/a_T in subsequent temperature steps of 5 °C and 3 min duration. a) 85/15 blend (start at 190 °C); b) 60/40 blend (start at 170 °C); c) 40/60 blend (start at 160 °C); d) 15/85 blend (start at 160 °C).

Table 12. Phase separation temperature from light microscopy

PαMSAN / PMMA	T_{ps} [°C]
85/15	190
60/40	175
40/60	165
15/85	< 160

For the 15/85 blend a decrease of transmission is observed already for the lowest temperature chosen which indicates that the limit of miscibility must be below 160 °C. Taking this into account a satisfactory agreement of the data from Tables 11 and 12 may be stated. Fig. 6 contains a plot of these data.

8. CONCLUSION

The selected blend system offers the possibility to prepare a variety of blend morphologies at constant composition. Starting from a miscible blend by squeezing below 160 °C droplet morphologies and co-continuous structures of different length scales may be obtained for the 40/60 and 60/40 mixtures, depending on the annealing conditions. The 15/85 and 85/15 blends only yield droplet morphologies. The morphology of the melt may be preserved by cooling below the glass transition temperature for subsequent characterization, e.g. by electron microscopy of RuO_4-stained ultrathin sections.

Since the viscoelasticity of the pure components at 210 °C is very similar - except for the factor of 0.61 in the time scale - the elasticity and viscosity functions of the constituents are very similar, too. This provides the unique opportunity to study the influence of the morphology on rheological properties without superimposition of effects that are mainly due to different flow properties of the two separate phases. Furthermore, the quite similar temperature shift factors enable to cover a wide range of time scales by varying the temperature again with minor changes of the phase properties.

ACKNOWLEDGEMENTS

The co-ordinator is indebted to his colleague W. Heckmann for providing the RuO_4-stained electron micrographs and to J. Rieger and I. Hennig for DSC data. G. Schmidt is thanked for the support in preparing the figures. We are grateful to L.A. Utracki for valuable suggestions that helped to improve the manuscript.

REFERENCES

1 Utracki, L.A. *Polymer Alloys and Blends: Thermodynamics and Rheology*. Munich, Vienna, New York: Hanser, 1989.

2 Goh, S.H., Paul, D.R. & Barlow, J.W. *Polym. Eng. Sci.* 1982, **22**, 34.

3 Koster, C., Altstädt, V., Kausch, H.H. & Cantwell, W.J. *Polymer Bulletin* 1995, **34**, 243–248.

4 Schytt, V. & J. Lyngaae-Jörgensen. *Polym. Networks Blends* 1997, **7**, 77.

5 McMaster, L.P.. In: *Copolymers, Polyblends and Composites*, p. 43.

6 Meissner, J. *Rheol. Acta* 1975, **14**, 201.

7 Baumgärtel, M. & H. H. Winter. *Rheol. Acta* 1989, **28**, 511.

8 Cox, W.P. & E.H. Merz. *J. Polym. Sci.* 1958, **28**, 619.